

## Wear Properties of Additively Manufactured Stainless Steels for Nuclear Components

Junhyun Kwon<sup>a</sup>, Jung-Min Kim<sup>a</sup>, Hyung-Ha Jin<sup>a</sup>

<sup>a</sup>Korea Atomic Energy Research Institute, 989-111 Daedeok-daero, Daejeon, 34057, KOREA

\*Corresponding author: jhkwon@kaeri.re.kr

### 1. Introduction

The two most commonly-used methods for laser-based metal additive manufacturing (AM) technology today are powder bed fusion (PBF) and directed energy deposition (DED). Each process has its own strengths and can be used for similar projects. PBF system uses a laser to selectively melt a bed of metallic powder layer by layer to build up the part. The PBF method is better at making smaller, more complicated parts, and produces a better surface finish. DED system continuously blow powder through nozzles directed at the focal point of a laser. The DED method is known to be faster and better at adding material to existing parts, which enables to repair the damaged components [1].

Recently, metal AM technology has been drawing interest in a nuclear industry. There are a number of potential applications for AM in the nuclear sector, including replacement parts for operating reactors and structural prototypes for next generation nuclear systems. Austenitic stainless steel (SS) 304L is used extensively for components both inside and outside the reactor pressure vessel. In this study, we are primarily investigating microstructure and wear properties of AM SS 304L which are made by the PBF and DED methods. Various properties of newly-manufactured alloys need to be defined for nuclear use, which will be available in the near future.

### 2. Experimental Procedure

#### 2.1 Materials and Processing Methods

Depending on the AM methods, we prepared SS 304L metallic powder as a feedstock with different sizes. In the PBF process, the sample was produced using spherical SS powder with an average particle size between 15 to 45  $\mu\text{m}$  in diameter, which was supplied by Chang Sung Corporation (Korea). The apparent density of the powder is 3.97  $\text{g}/\text{cm}^3$ . SS 304L specimens were made using a commercial PBF equipment (Laser CUSING, Concept Laser). In this process, metallic powder is spread in thin layers with a layer thickness of 30  $\mu\text{m}$  across a work area. For uniform distribution of the powder a leveling blade is used. A fiber laser beam with a power of 180W is directed with a scan speed of up to 800 mm/s across the deposited powder layer. Typical spot size of the laser beam in the focal plane is between 50 and 150  $\mu\text{m}$ . The PBF process is carried out in a closed process chamber in which an inert gas

atmosphere is continuously maintained, so the residual oxygen content is less than 0.5 %. Argon is fed into the chamber to avoid undesired interactions of the metal powder with its environment and to protect the melt.

In the DED process, we used the SS 304L powder provided by CARPENTER (USA), which has a particle size of 45 to 150  $\mu\text{m}$  and an apparent density of 4.34  $\text{g}/\text{cm}^3$ . SS 304L specimens were manufactured using a commercial DED equipment (MX-400, InssTek). A part is built by means of melting a surface and applying the metal powder simultaneously. In contrast to the PBF process, DED provides a high buildup rate and allows for relatively larger volumes. In the DED process, we can obtain build rates up to 5.5  $\text{cm}^3/\text{h}$ . Feed rates of 2.5 to 3.0  $\text{g}/\text{min}$  are employed for the deposition of metal powder. The spot size of the laser beam varies between 0.8 and 1.0 mm and the scan speed reaches up to 850 mm/min. [Both PBF and DED samples were produced in rectangular bars with size 125 x 60 x 30 mm.](#)

#### 2.2 Microstructure Observation

SS 304L specimens, made by the PBF and the DED process, were prepared for microstructure observation. Macro- and micro-structure characterizations were carried out on the etched surface both by an optical microscope (OM) and a scanning electron microscope (SEM). We investigated the pore distribution and grain structure from the OM images of the cross section view of the specimens. The detailed sub-grains were observed by SEM.

#### 2.3 Wear Tests

Prior to wear tests, hardness measurements for the AM SS 304L samples were performed using a micro-hardness tester (HM-122, AKASHI) with a load of 1 kgf. We measure the hardness on a face parallel to the building direction at regular intervals upward from the baseplate and compare them with that of wrought SS. [Tensile tests on the AM samples are currently underway. The results will be available in the near future.](#)

The sliding wear tests on SS 304L were carried out based on the ASTM standard G99, which is titled as 'Standard test method for wear testing with a pin-on-disk apparatus' [2]. The test rig consists of a vertical pin, 5 mm in diameter, loaded against a horizontal rotating disk, 30 mm in diameter. The nominal applied load was 30 N, and sliding velocity was kept at about 0.22 m/s. The tests were carried out for a sliding distance of 1.6

km at two different temperatures, 25 and 250°C. The degree of wear was determined by measuring the weight loss of specimens before and after the tests.

### 3. Results

#### 3.1 Microstructure Characterization

The microstructure of alloys is strongly dependent on their production methods. The same alloys made by a different route can manifest different microstructure, which eventually lead to distinct mechanical behaviors. First, we observed the grain structures of SS 304L made by the PBF and DED methods. The microstructure of the PBF samples is shown in Figs. 1 (a) and (b) from OM and SEM, respectively. The OM image shows a semicircular pattern with an average size of 100  $\mu\text{m}$  in diameter, which is called a melt pool. Fine cellular sub-grains were distributed sporadically, which could be seen in the SEM image. In the DED samples, larger melt pools in a semicircular shape were observed and relatively coarse cellular sub-grains were seen with a high density, which are shown in Figs. 1 (c) from OM and (d) from SEM.

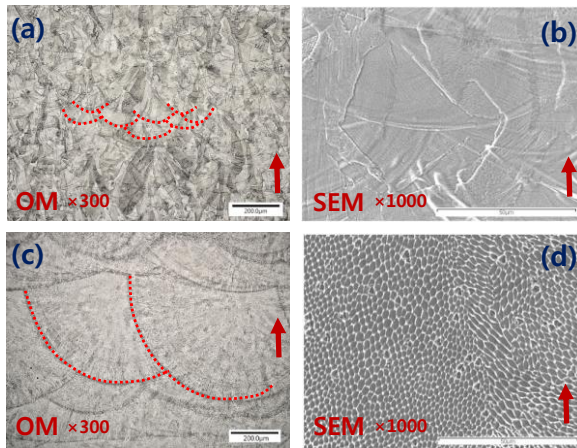


Fig. 1. OM and SEM images of AM SS 304L samples, all cross-section parallel to material build direction: (a) OM – PBF, (b) SEM – PBF, (c) OM – DED, (d) SEM – DED.

It is known that the presence of residual porosity in AM parts affects their mechanical properties. Hence, we evaluated the pore distribution in the AM samples by observing the OM images. Fig.2 shows the optical images of cross sections of vertically-oriented samples in which pores are clearly visible. In the PBF sample, we could observe higher porosity and larger pore size. The results of the porosity analysis are listed in Table 1. It is of our interest to understand the effect of pore distribution on the mechanical behaviors of AM materials.

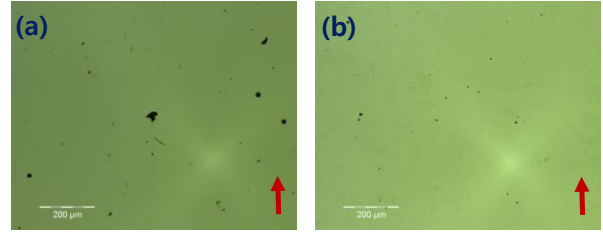


Fig. 2. Optical view of vertical cross sections of AM SS 304L: (a) PBF, (b) DED.

Table 1: Pore analysis of AM SS 304L samples manufactured by PBF and DED methods

	Areal pore fraction (%)	Average pore density (#/mm <sup>2</sup> )	Max. pore diameter ( $\mu\text{m}$ )
PBF	0.14	83	6.81
DED	0.05	41	4.04

#### 3.2 Wear Properties

The measured Vickers hardness data for SS 304L specimens were listed in Table 2. The hardness from AM SS 304L was obtained by averaging the measured values. The average hardness values for two AM SS were higher than that for wrought SS and the hardness for the DED sample was highest among the specimens.

We measured the total weight loss of three SS 304L samples from the pin-on-disk sliding tests, which are summarized in Fig. 3. For testing conditions described in the previous section, the DED sample shows the highest wear resistance, implying the lowest wear amount. The DED specimen displayed higher hardness as compared to other ones in this work, which is related to the wear resistance [3]. The wear test results show that the wear resistance is proportional to the hardness values, which is in agreement with the Archard wear equation [4]. It is also found that the weight loss diminished significantly as temperature increases. This finding is linked to the difference in wear mechanisms. At high temperature, metal surfaces tend to be covered with a thin layer of film. This film prevents direct metallic contact, which eventually reduces the amount of sliding wear [5].

Table 2: Vickers hardness of three SS 304L samples (wrought, PBF, DED)

	Wrought	PBF	DED
Vickers Hardness (VH)	204.0	218.4	246.4

### 4. Conclusions

In a nuclear industry, it is challenging to apply the AM products to a system. While AM SS has achieved a significant success with near full density, reasonable

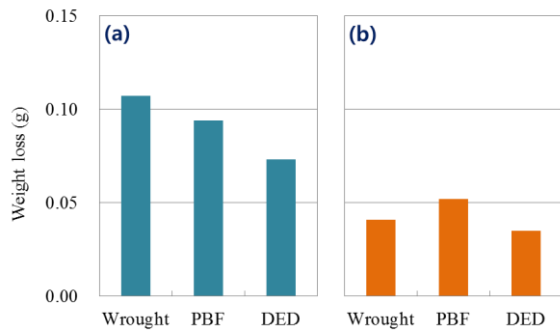


Fig. 3. Weight loss depending on the manufacturing method of SS 304L, including conventional, PBF and DED processes. (a) at 25°C and (b) at 250 °C.

microstructure and suitable tensile properties, little work has been done to evaluate the materials requirements for nuclear applications. We consider AM SS 304L as reactor structural materials which are required for wear resistance. Hence, wear properties in SS 304L made by two AM methods, PDF and DED, were evaluated, as well as microstructural analysis. From this work, the following facts were found

- AM SS 304L contained a certain amount of macroscopic defects (pores, cracks, sub-grains *etc.*) and microstructural features (unrecrystallized grains, precipitates *etc.*) for both PBF and DED samples.

- Wear test results show that AM SS 304L exhibited better wear resistance at a room temperature as compared to commercial SS. In particular, DED SS shows the prominent wear resistance at both room and high temperature.

## REFERENCES

- [1] Wohlers Report 2017, 3D printing and additive manufacturing state of the industry annual worldwide progress report, Wohlers Associates, USA, 2017.
- [2] ASTM G99-17, Standard test method for wear testing with a pin-on-disk apparatus, ASTM Int., USA, 2017.
- [3] F. Bartolomeu, M. Buciumeanu, E. Pinto, N. Alves, O. Carvalho, F.S. Silva, and G. Miranda, 316L stainless steel mechanical behavior – A comparison between selective laser melting, hot pressing and conventional casting, Additive Manufacturing, Vol. 16, p.81, 2017.
- [4] I. Hutchings and P. Shipway, Tribology: Friction and Wear of Engineering Materials, 2<sup>nd</sup> Ed., B-H Publishing, 2017.
- [5] S.C. Lim, The relevance of wear-mechanism maps to mild-oxidational wear, Tribol. Int., Vol.35, p.717, 2002.